Int. J. Rock Mech. Min. Sci. Vol. 9, pp. 161–182. Pergamon Press 1972. Printed in Great Britain

VOLUME CHANGES DURING THE DEFORMATION OF ROCKS AT HIGH PRESSURES

J. M. EDMOND and M. S. PATERSON

Department of Geophysics and Geochemistry,
Australian National University,
Canberra, Australia

(*Received* 30 *May* 1971)

Abstract—Using a dilatometric method, volume changes were measured during straining to 20 per cent at confining pressures up to 8 kb, as well as during application and release of the pressure, in lithographic limestone, Carrara marble, sandstone, talc, graphite and sodium chloride. Dilatancy persists well into the ductile field but compaction tends to occur during straining at the higher pressures. In some cases, notably sandstone, compaction can be followed by dilation as straining continues. The stress–strain curves are shown to be significantly affected by the occurrence of volume changes because of the work done through them by the confining pressure. Therefore, an alternative flow parameter, defined as the total rate of doing work on the specimen with respect to strain, is considered to be a better guide in deducing from stress–strain behaviour the relative roles of cataclastic flow and intracrystalline plasticity as mechanisms of deformation. The brittle–ductile transition is seen as the pressure above which unstable propagation of microcracks no longer occurs, the transition to complete intracrystalline plasticity occurring at a higher pressure, if attained at all.

INTRODUCTION

NON-ELASTIC volume changes can occur during the deformation of a rock without macroscopic fracturing being involved. They may reflect fine-scale fracturing, changes in pore structure or other internal structural changes in the rock. These changes are intimately associated with the mechanism of deformation, especially in the transition between brittle and ductile behaviour, as well as with the processes leading up to macroscopic fracture. The measurement of volume changes can therefore make an important contribution to our understanding of the details of the response of a rock to applied stress.

The first accurate measurements were made by BRIDGMAN [1], using a dilatometric method. In some rocks of low porosity he observed volume increases prior to fracture in uniaxial compression at atmospheric pressure. BRACE, PAULDING and SCHOLZ [2, 3] have made more detailed studies of volume changes prior to fracture in a number of rocks tested under high pressure, using a strain-gauge method. This and related work of Brace and co-workers has thrown much light on the microfracturing that precedes macroscopic fracture but its application has been mainly in the brittle field and at small strains.

Very few measurements have been made of volume changes during the larger strains that rocks can undergo in the ductile field at high pressures. Notable here is the work of HANDIN and co-workers [4, 5]. By measuring the movement of pore fluid in or out of the specimen in triaxial compression tests at constant pore pressure, they observed decrease in volume during deformation of rather porous limestone and sandstone and increase in volume, after an initial decrease, in a dolomite of lower porosity; at very low effective pressures, all specimens dilated. The highest effective pressure used was $1 \cdot 5$ kb. The same method was used by BRACE and ORANGE [6] at small strains and it is widely used in soil mechanics. It is limited in application by the requirements of adequate permeability and interconnexion of pores, requirements not met in many compact rocks as HANDIN *et al.* [5] showed in the case of a shale and BRACE and ORANGE [6] in marble.

In the present study, a dilatometric method has been used to measure volume changes during deformation in rocks at confining pressures up to 8 kb. The aim has been to throw further light on the mechanisms involved in the brittle to ductile transition and to help determine the relative contributions of cataclastic and crystal–plastic deformation mechanisms at pressures above the transition. This is of interest in view of the difficulty of achieving intracrystalline deformation in a polycrystalline aggregate if an insufficient number of active slip systems is available in the individual grains (cf. von Mises' requirement of five independent slip systems [7–9]). The implications of the von Mises' requirement for ductility in rocks are discussed elsewhere [10].

APPARATUS AND EXPERIMENTAL METHOD

The measurements were made with a new device which fits into the high-pressure cylinder of a 10-kb room temperature deformation apparatus described elsewhere [11]. In principle, the jacketed specimen is enclosed within a fluid-filled bellows and volume changes in the specimen, which cause displacement of the fluid, are indicated by relative movement of the ends of the bellows. This dilatometric method, like that of BRIDGMAN [1], integrates the volume changes over the whole specimen. In this respect, it is similar to the pore fluid method but it has the advantage of being independent of the permeability of the specimen. It has the advantage over the strain-gauge method of not requiring elaborate preparation for each experiment and it is not restricted to relatively small strains.

The dilatometer is depicted schematically in Fig. 1 and in section in Fig. 2. The overall dimensions are 1¼ in. diameter and 5½ in. length, set by the dimensions of the pressure

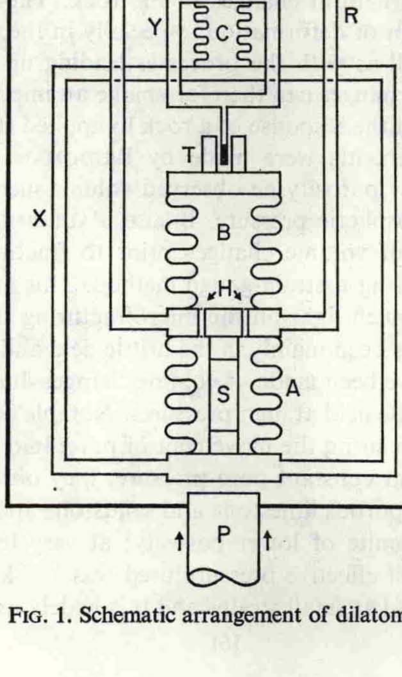

FIG. 1. Schematic arrangement of dilatometer.

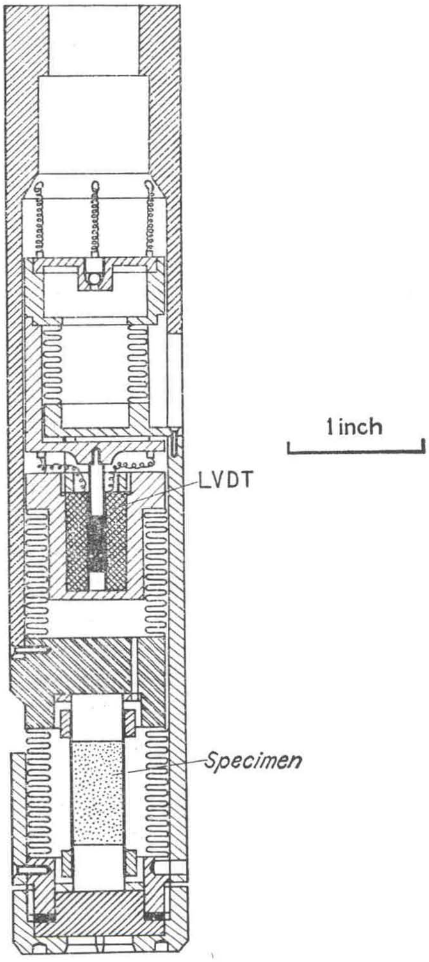

FIG. 2. Cross section of dilatometer.

vessel. The specimen *S* is enclosed in bellows *A* which is filled with water, chosen because of its low compressibility (sodium dichromate is added to inhibit corrosion). The piston *P* applies compressive load to the specimen and the reaction is provided by anvil *R* to which one end of bellows *A* is fixed. Movement of the free end of bellows *A* displaces fluid through interconnecting holes in *R* to an identical bellows *B* attached to the other side of *R*. The displacement of the free end of bellows *B* is therefore identical to that of *A* unless there is volume change in the specimen. The free ends of bellows *A* and *B* are connected, via a yoke *X* and pressure compensator, to the core and body, respectively, of a linear variable differential transformer (LVDT, supplied 'unpotted' by Schaevitz Corp., U.S.A., so as to be suitable for operation in the high-pressure fluid). The signal from the LVDT is then proportional to the volume change in the specimen. The signal is taken from the pressure vessel through two insulating seals in the top closure and power is supplied to the LVDT through another two seals.

Since the water in the dilatometer is itself compressible, pressure fluctuations would also tend to be registered due to the corresponding relative movement of the free ends of bellows *A* and *B*. To avoid this, a pressure-compensating device is incorporated, consisting of a bellows *C* and another yoke *Y* (Fig. 1). By carefully adjusting the volume of water in bellows *C* relative to that in *A* and *B*, the pressure compensator will give a displacement that is exactly equal and opposite to the relative displacement of the free ends of the bellows *A* and *B* due to the volume change in the water in them, thus ensuring that there is no signal from the LVDT. This permits direct measurement of volume changes in the specimen during raising and lowering of the pressure as well as ensuring freedom from spurious signals due to small pressure fluctuations during the deformation.

The specimens for compression tests are 10 mm in diameter and 20 mm long. They are sealed inside an annealed copper jacket of 0·25 mm wall thickness, closed at each end by a steel end-piece; force-fitted steel rings effect the seal between the copper and the steel end-pieces. Extension tests can also be done by replacing the compression test assembly by an interpenetrating double-yoke arrangement into which a smaller specimen (7 mm diameter, 13 mm length) can be fitted, sealed in a copper jacket soldered at its ends to the yokes.

The pressure medium in the pressure vessel was kerosene except at 8 kb when petroleum ether was used on account of its lower viscosity. Volume-change experiments at pressures above 8 kb were not attempted because the water in the dilatometer would freeze at about 9 kb. The strain rate was about 4×10^{-4} sec^{-1} in all tests.

Calibration tests using carbide or copper specimens enabled a small correction to be determined for the effect of slight mis-match of the supposedly identical bellows and adjustment made of the correct amount of water in the pressure compensating bellows. The volume changes in the specimen are obtained by calibrating the LVDT signal as a displacement by connecting the LVDT directly to the piston *P* and then multiplying by the effective cross-sectional area of the bellows. In compression tests, the overall accuracy is believed to be $\pm$ 0·01 in per cent relative volume change, while in extension tests, because of the specimens being smaller, it is about $\pm$ 0·02 per cent, but, as noted later the scatter between specimens tended to exceed these figures. Also, during increase or decrease of confining pressure, somewhat greater errors, of the order of $\pm$ 0·02 and $\pm$ 0·04 per cent, respectively, could occur over most of the range, with even greater uncertainty at very low pressures, probably due to the presence of some air bubbles and to the collapse of the imperfectly fitting copper jackets.

After the experiments, the bulk density of the specimens was determined with a sensitivity of about 1 part in 1000 by weighing in air and under water after a thin coating of paraffin wax had been applied. This provided a check on the measured final volume change. The initial densities of the specimens was determined in the same way (Table 1).

The experiments were performed in triplicate except where otherwise stated. The method of reducing the stress–strain data has been described earlier [11]. In brief, strains are expressed as percentage change of length, referred to the initial length measured at atmospheric pressure; apparatus distortion is allowed for. Stresses are calculated from the load, corrected for friction (an external load cell was used), and are based on the cross-sectional area at the given strain, assuming that the strain has been uniform and neglecting all volume changes. The stress quoted is the 'differential stress', that is, axial stress minus the confining pressure. The errors in stress–strain measurements [11] are small generally compared with the scatter in results between specimens except in the early parts of the curves (up to about 1 per cent strain) where the errors may be considerable.

MATERIALS

The rocks and other materials studied are listed in Table 1. In the case of the sandstone and talc, all specimens were cored from single blocks in the same direction. Similarly all graphite specimens were turned from a single rod; X-ray texture goniometer measurements on it showed that about three times as many crystals had their basal planes parallel to the specimen axis as perpendicular to it. The sodium chloride specimens were fabricated with a standardized procedure in a piston–cylinder press, using a nominal pressure of 10 kb; they were not annealed since it was desired to reproduce possible conditions of usage in solid-medium high-pressure apparatus.

TABLE 1. MATERIALS STUDIED

Material	Density (gm cm^{-2})	Porosity† (per cent)	Remarks
Lithographic limestone	2·56	5·9	Fine-grained (about 0·01 mm); isotropic‡ presumed to be Solenhofen limestone
Carrara marble	2·69	1·1	Grain size about 0·1 mm; isotropic‡
Gosford sandstone (New South Wales)	2·45	13	Weakly cemented quartz and felspar (about 0·2 mm grain size) in matrix of clay and mica; slightly anisotropic‡
Three Springs talc (West Australia)	2·71	3·2	Fine-grained; nearly isotropic‡
Graphite	1·73	25	Electrographite Grade EY9, supplied as rod by Morganite Carbon Ltd (Australia); anisotropic (see text)
Sodium chloride	2·15	0·5	Analytical reagent grade; fabricated by pressing (see text)

† Calculated from measured bulk density and known single crystal density; in the case of the sandstone, the mean of quartz and felspar is used for the latter.
‡ Based on stress–strain curves measured on mutually orthogonal specimens.

In the case of the sodium chloride, the powder was dried before fabrication of the specimens, and in the case of the other materials several weeks of air-drying had been allowed before testing. Otherwise, no special precautions about moisture content were taken.

RESULTS

Lithographic limestone

The stress–strain curves are given in Fig. 3(a) for compression tests at confining pressures from 1 to 8 kb and for extension tests at 6·5 kb. The corresponding relative volume change vs strain curves are given in Fig. 3(c). In these and subsequent figures the line marked 'scatter' indicates the range of scatter amongst repeat experiments which applies approximately to all the curves shown, the curves giving the average results. The relative volume change $\Delta v/v_0$ plotted is referred to the initial volume v_0 measured at atmospheric pressure.

The brittle–ductile transition, as defined by the change from a sharply-defined narrow shear to a widely-distributed deformation, occurs between 1 and 2 kb confining pressure in compression and is accompanied by a change from turning-over to continually-rising

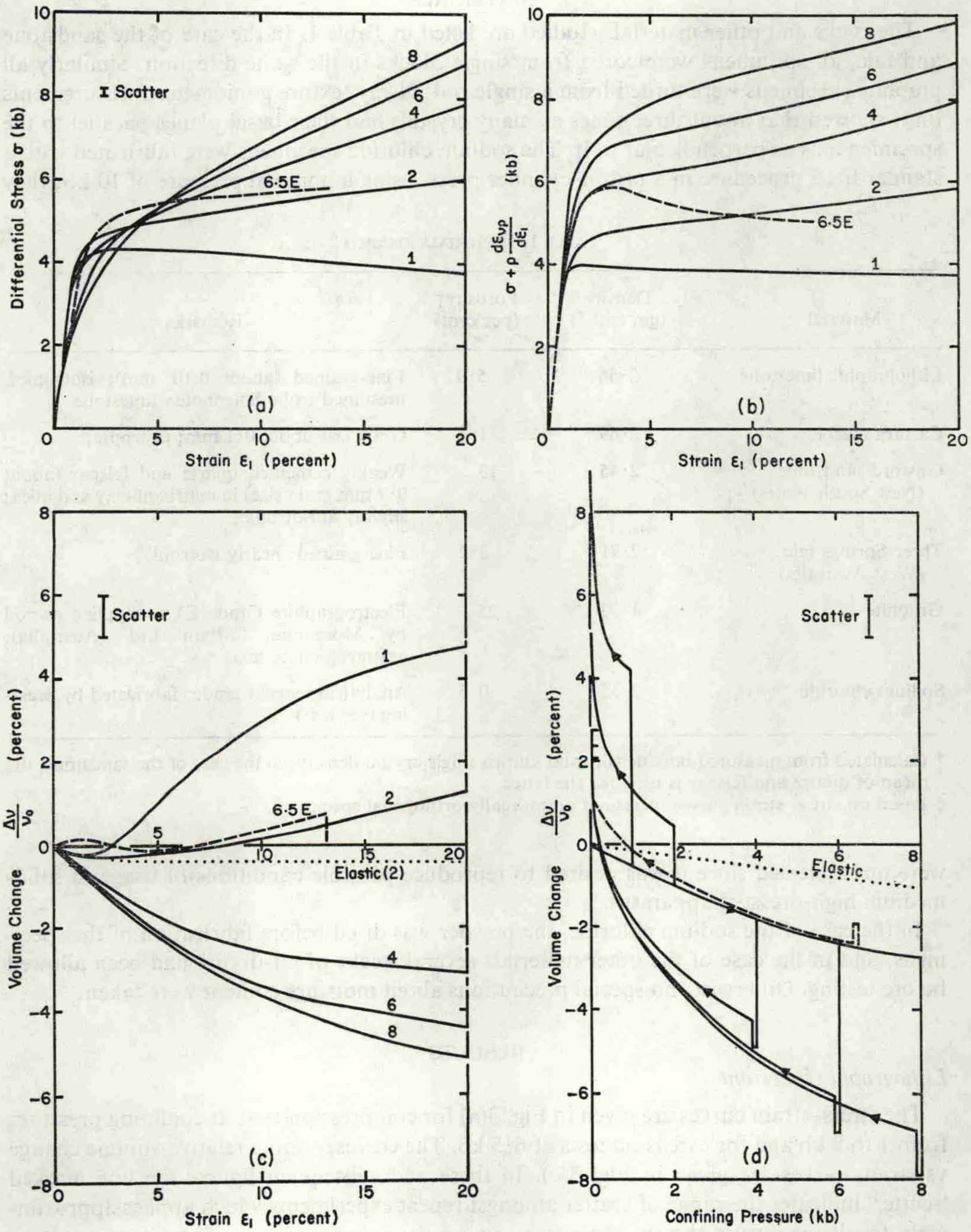

FIG. 3. Results for lithographic limestone: (a) stress–strain curves at confining pressures 1–8 kb (indicated on curves; 6·5 E is an extension test, all others in compression); (b) equivalent stress–strain curve calculated from total work done on specimen; (c) relative volume change vs strain at pressures indicated, corresponding to stress–strain curves in (a); (d) complete history of volume changes.

stress–strain curves. The unusual order of the compression stress–strain curves at low strains and the cross-over with increasing strain has been observed previously in this rock, as has also the relatively high level of the extension curve at low strains [11]; these effects will be discussed later in relation to the volume changes. The extension tests were terminated at about 13 per cent strain because of the onset of necking.

The most notable aspect of the volume change results in compression [Fig. 3(c)] is the change from dilatational behaviour at low pressures to compaction during straining at high pressures, similar to that observed by SCHOLZ [3] in marble up to about 2 per cent strain. The initial stage of slight volume decrease in compression at low pressures and the corresponding increase in extension is presumably largely an elastic effect. The dotted curve in Fig. 3(c) represents, as a typical case, the calculated elastic volume change during the straining at 2 kb confining pressure (the choice of elastic parameter is dealt with in the discussion). It is seen that in general the observed volume changes are large compared with elastic volume changes and must be attributed mainly to changes in porosity. Interpolation suggests that, in compression, deformation at approximately constant volume should take place at about 2·5 kb confining pressure and this has been verified experimentally. It was also noticed that barrelling was pronounced in specimens deformed below 2·5 kb whereas at higher pressures the specimens remained nearly cylindrical during deformation except in the immediate vicinity of the ends.

The complete histories of the volume changes are represented in Fig. 3(d), including those occurring during the application and removal of the confining pressures (see comment above on accuracy); the slightly separated vertical lines represent the changes occurring during the stress–strain test at constant confining pressure [Fig. 3(c)]. For comparison, the calculated elastic changes for pore-free polycrystalline calcite (based on the compressibility of single crystals) are indicated by the dotted line. It is seen that:

1. Even at 8 kb, much of the initial porosity remains after application of the confining pressure. Straining while under the higher pressures was much more effective in eliminating porosity. However, only at 8 kb was the initial porosity almost completely eliminated by the 20 per cent straining in compression.
2. Relatively large increases in volume occurred during pressure release. The rate of increase of volume increased markedly at the lower pressures and the total amount was greater the higher the pressure at which the deformation was done. In all cases, the final volume and porosity was greater than for the virgin material, the difference being more marked when the pressure applied was lower.
3. The volume changes during pressure release after the extension tests at 6·5 kb confining pressure were notably less than those observed after compression tests.

Carrara marble

The stress–strain and volume change–strain curves are given in Figs 4(a) and 4(c) and the volume change–confining pressure curves for the whole experimental sequence are given in Fig. 4(d). While the behaviour is in many respects similar to that of the lithographic limestone, the following differences are to be noted:

1. The brittle–ductile transition pressure is lower, between 0·5 and 1 kb.
2. The stress–strain curves are generally lower, with no crossing over, and the effect of pressure between 6 and 8 kb is less.
3. The tendency for volume to increase during straining persists to higher pressures, presumably because of the lesser role played by elimination of the much smaller

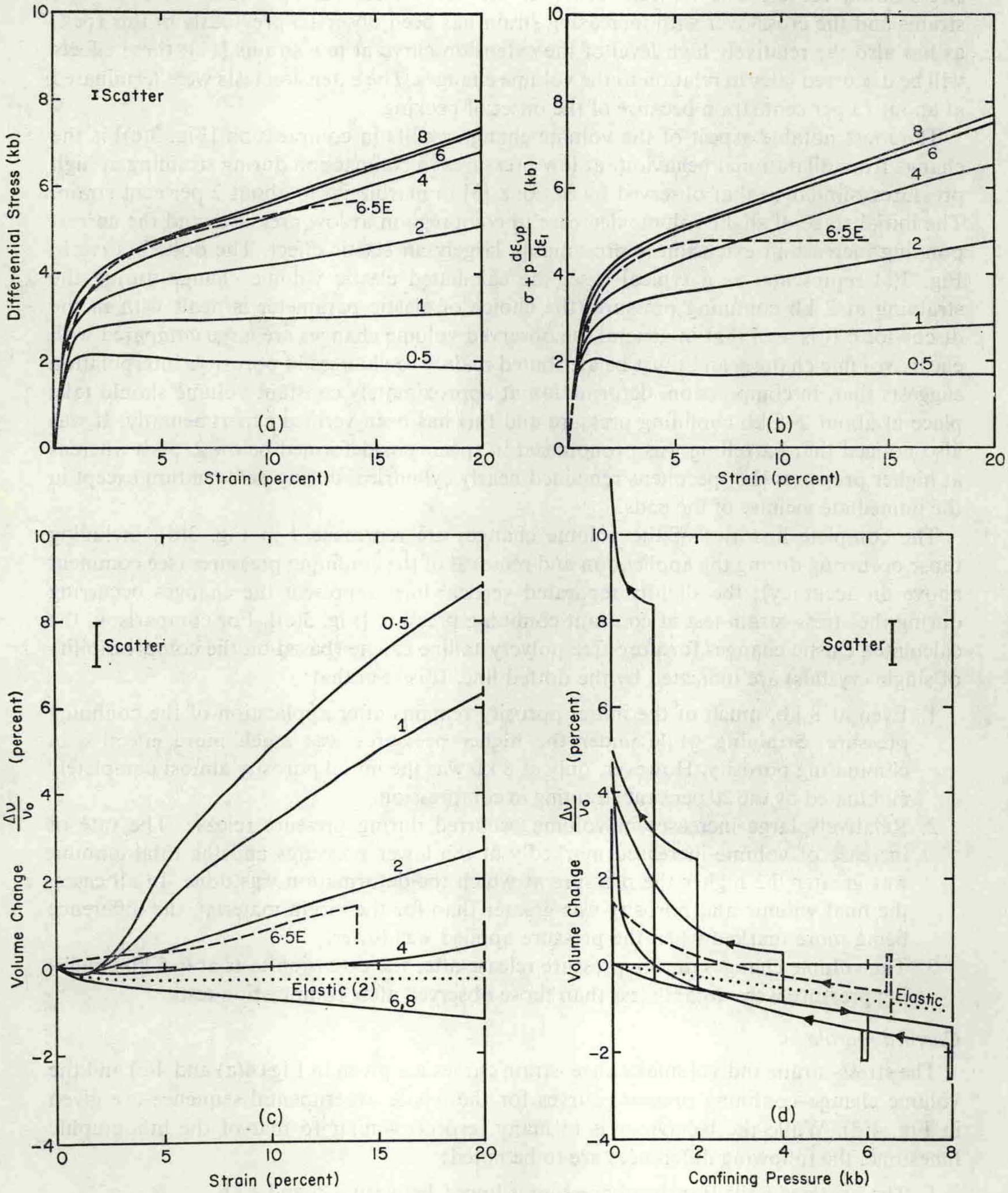

FIG. 4. Results for Carrara marble (cf. caption to Fig. 3).

initial porosity. Again, the small decrease in volume which precedes predominantly dilatant behaviour is probably largely elastic. Again, also, specimens which dilated during deformation were observed to be notably barrelled whereas specimens which had deformed with no change or a decrease in volume were almost cylindrical.

4. The increases in volume during pressure release, while similar in trend, were significantly smaller in magnitude than in the limestone.

Gosford sandstone

The stress–strain and volume change results for the sandstone are given in Figs 5(a), (c) and (d). Measurements were made only to 6 kb because the loads required to deform the sandstone at higher pressures might have overloaded the dilatometer. Also only compression tests were done on this and the subsequent materials.

All the stress–strain curves reached or passed through a maximum and the flow stress increased markedly with pressure over the whole pressure range. A brittle–ductile transition is less clearly defined in terms of specimen appearance than in the calcite rocks but the absence of a single discrete shear fracture places the behaviour as ductile. After 20 per cent deformation, however, all specimens showed some degree of non-uniform deformation, in addition to localized end effects. At 1-kb broad conjugate shear bands appeared, while at higher confining pressures specimens barrelled in a somewhat irregular manner without showing distinct shear zones. However, specimens strained only 10 per cent at 4 and 6 kb appeared to be uniformly deformed.

At all pressures, straining led first to a compaction of the specimen and subsequently to a dilation, although the initial compaction at 1 kb is probably mainly an elastic effect. A notable feature of the measurements was a large scatter between specimens (especially at 2 kb), as a result of which it is doubtful whether the differences shown between the mean curves for the three higher pressures [Fig. 5(c)] are significant. However, the change from compactional to dilational behaviour during straining was consistently present. The observation differs from observations on unbonded sand at moderate pressures (up to the order of 1 kb) in which only compaction during straining is observed [12, 13] although there is a suggestion of the effect at 1·5 kb effective pressure [5]. As for the calcite rocks, substantial non-elastic volume increases occurred during pressure release, larger at higher pressures, and leading in all cases to a final porosity greater than the initial [Fig.5(d)].

Three Springs talc

The measurements are given in Figs 6(a), (c) and (d). Specimen appearance suggested a brittle–ductile transition at about 4 kb, corresponding to the change to continually rising stress–strain curves. As for the previous materials, all specimens decreased in volume at first during straining, probably mainly elastically, followed by considerable dilation at 2 and 4 kb, approximately constant-volume deformation at 6 kb and slight further compaction at 8 kb [Fig. 6(c)]. Barrelling was minimal at 6 and 8 kb. Considerable non-elastic volume increases, larger at higher pressures, occurred in all cases during pressure release, giving a final porosity greater than the initial [Fig. 6(d)]. Further stress–strain studies, at high temperatures and on other talcs, are reported elsewhere [14].

Graphite

The behaviour of graphite is discussed in detail elsewhere [15] but the results are given in Figs 7(a), (c) and (d) for comparison with the other materials. The brittle–ductile transition

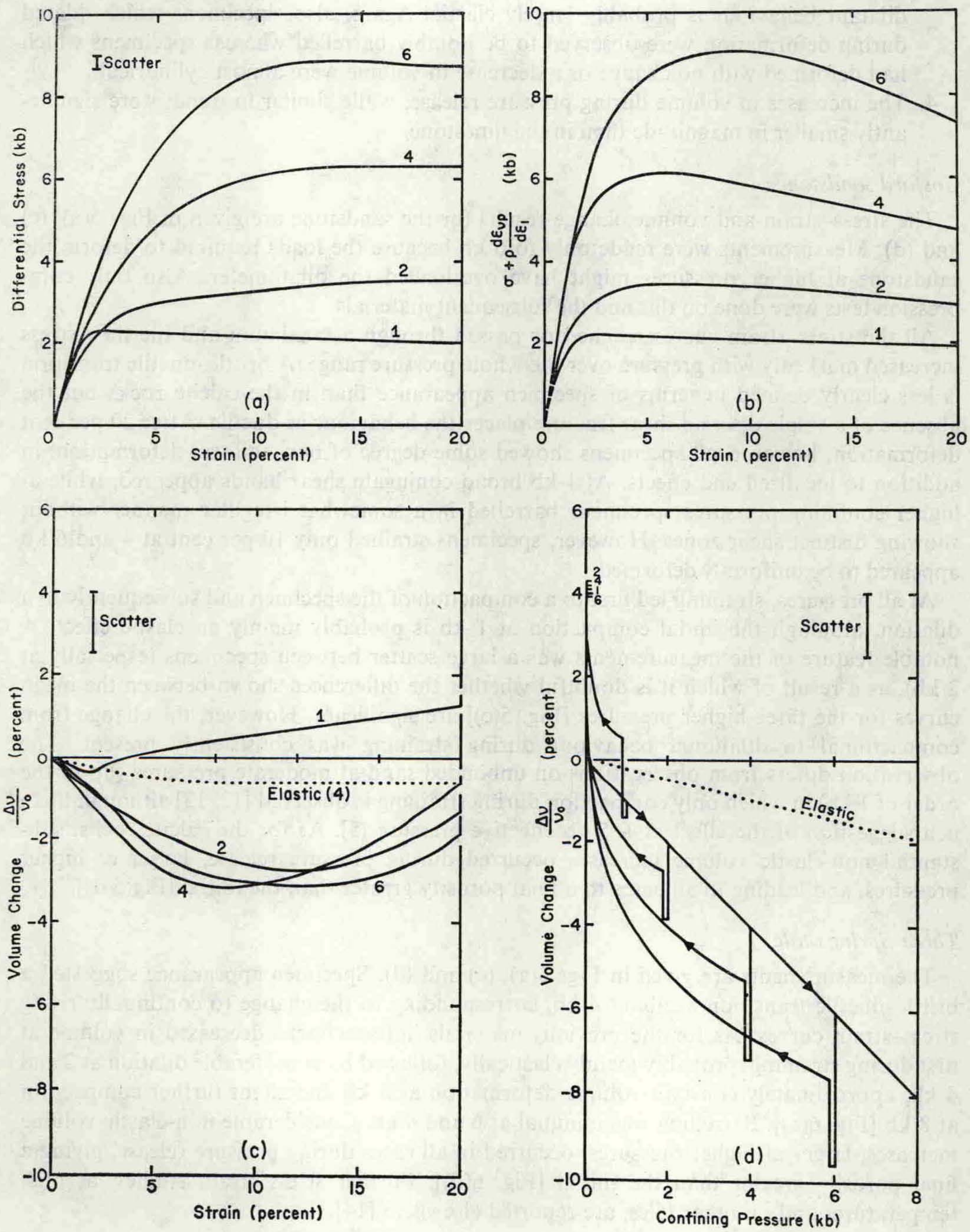

FIG. 5. Results for Gosford sandstone (cf. caption to Fig. 3).

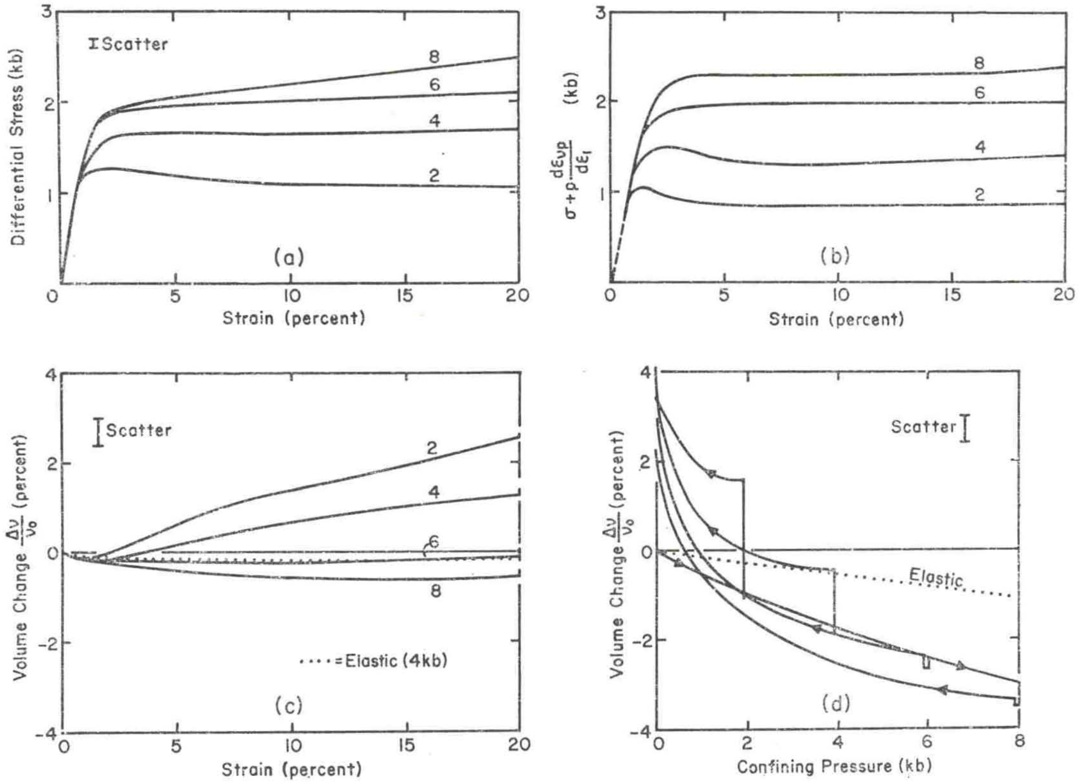

FIG. 6. Results for talc (cf. caption to Fig. 3).

is between 0·5 and 1 kb. The behaviour of graphite is remarkable for the following anomalies when compared with the other materials:

1. It compacts during deformation at all pressures but to a *lesser* degree at higher pressures; this is presumably related to the large degree of compaction under pressure alone.
2. During pressure release and the accompanying volume expansion, after 20 per cent deformation, the original length is almost completely recovered as well as the original volume, that is, the shape recovered too so that to the eye the specimens appeared undeformed. Also a large part of the recovery occurred below 0·5 kb.

Sodium chloride

Two specimens were deformed at each of the confining pressures 0·25, 0·5, 1, 2, 6 and 8 kb. Within the scatter indicated, no effect of pressure on the stress–strain curve was detected [Fig. 8(a)]. There was a small volume decrease, in excess of elastic change, during deformation at each pressure [Fig. 8(c)]; again, within the scatter of results, no clear difference at different confining pressures was detected although there was tendency for the volume decreases to be smaller at higher pressures. The latter effect is probably real, corresponding to the greater degree of elimination of porosity at higher pressures during

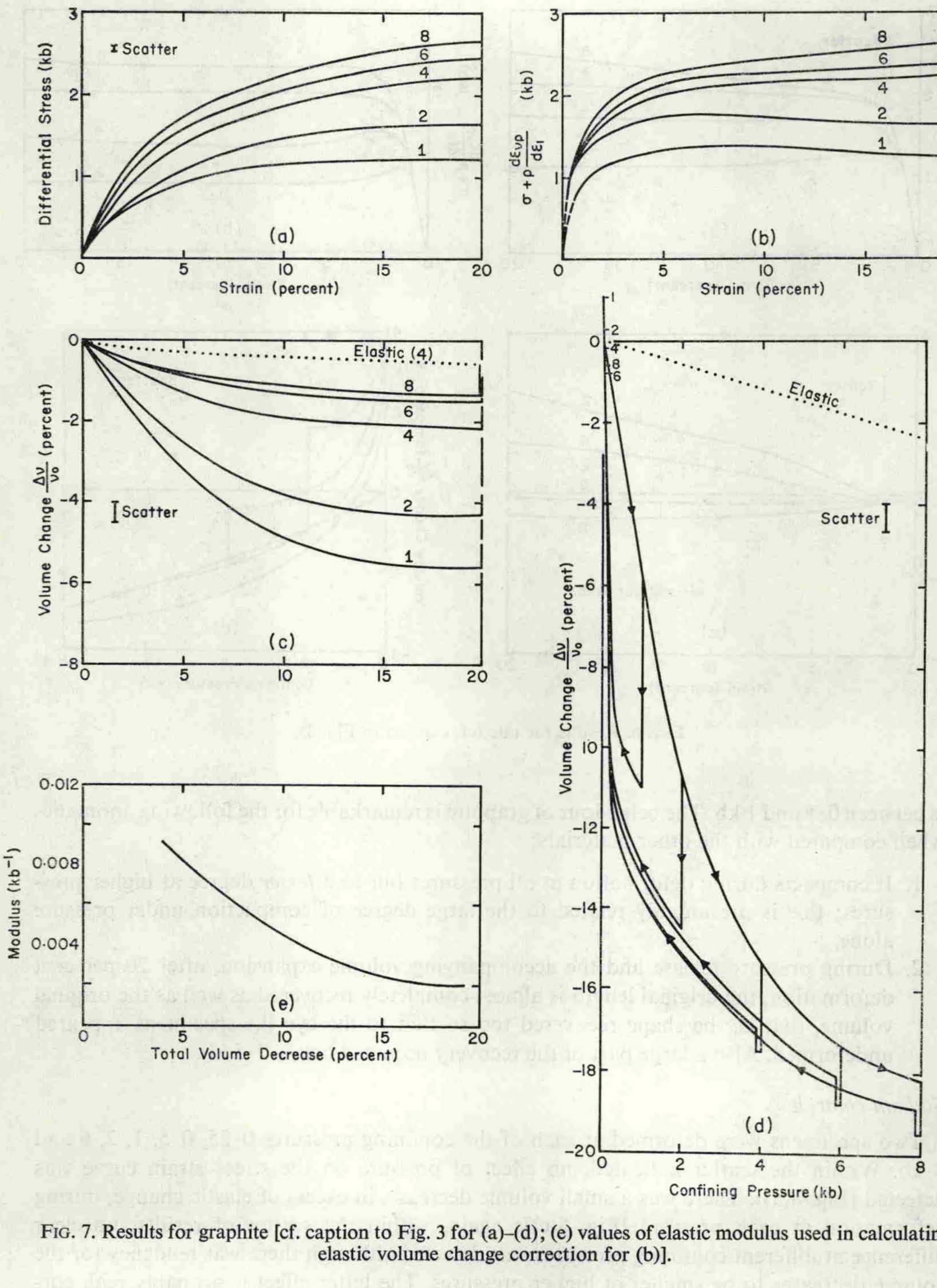

FIG. 7. Results for graphite [cf. caption to Fig. 3 for (a)–(d); (e) values of elastic modulus used in calculating elastic volume change correction for (b)].

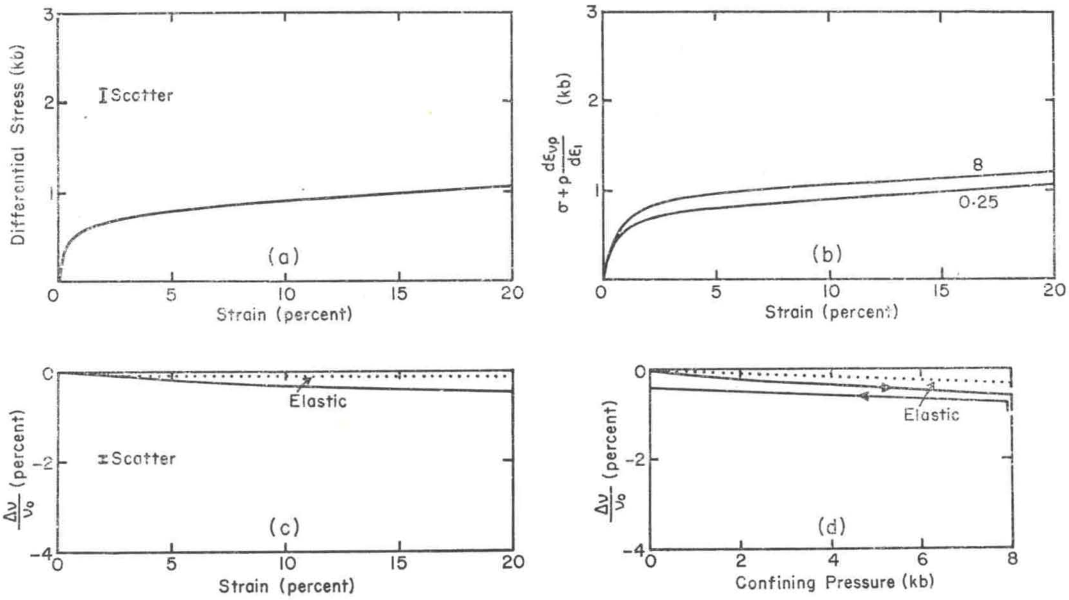

FIG. 8. Results for sodium chloride: (a) stress–strain curve, same within limits of scatter for 0·25, 0·5, 1, 2, 6 and 8 kb; (b) equivalent stress–strain curves for 0·25 and 8 kb calculated from total work done on specimens; (c) relative volume change vs strain, same within limits of scatter for 0·25, 0·5, 1, 3, 6 and 8 kb; (d) complete history of volume changes.

initial application of the pressure [Fig. 8(d)], since the final porosity of the specimens was in all cases less than 0·1 per cent, as determined by density measurements. Thus, the small initial porosity was effectively eliminated by the combined effects of confining pressure and deformation at all pressures and the changes in volume during pressure release were purely elastic.

DISCUSSION

General

The experiments have shown that the deformation of rocks can be accompanied by substantial volume changes even in the range of macroscopically ductile behaviour, thus confirming and extending previous observations [3, 5]. These volume changes are large compared with elastic effects and must be attributed to changes in the pore structure or grain arrangement or to the development of internal cracking. They may be of either sign, so presumably there are competing processes of compaction and dilation, especially where initial porosity is present. We shall first discuss some general aspects of the observations, then consider in more detail the interaction between volume changes and stress–strain properties, and finally attempt to draw conclusions about the mechanisms of deformation.

There is no obvious general correlation between the brittle–ductile transition and any particular aspect of the volume-change behaviour, such as change from dilation to compaction or the disappearance of non-elastic volume change. Thus, in the simplest case of Carrara marble, dilation can still accompany deformation above the brittle–ductile transition and it is not until much higher pressures that constant-volume deformation at zero porosity is achieved, like that in a ductile metal. However, there is some correlation between volume change during deformation and the pressure-sensitivity of the stress–strain curve. Where the latter is low, as for limestone and marble at the highest pressures and for sodium chloride at all pressures, the occurrence of volume change during deformation is minimal, probably only involving the elimination of some residual porosity.

The marked dilation of most materials during pressure release can be related to earlier observations on the increase of length during pressure release [16]. The limestone, marble and sandstone used here resemble fairly closely the corresponding materials used in the earlier work and it is probably valid to make rough comparisons. Thus, the total dilation during pressure release from 6 or 8 kb after deformation in these three materials is approximately 9, 6 and 12 per cent, respectively, while the total length increase during similar pressure release is 4·5, 4 and 4 per cent (based on original lengths for valid comparison). It follows that the pressure-release effects in the calcite aggregates is expressed predominantly as an increase in length, especially in the case of the initially more compact marble, whereas the dilation of sandstone is more nearly isotropic. This is consistent with the special mechanism, involving the plastic and elastic anisotropy of the grains, postulated for the calcite aggregates [16] and with the absence of these factors in sandstone. In the latter, the dilation during pressure release presumably results mainly from a general loosening of the granular structure under the influence of contact stresses set up during deformation at the high pressure and differing from those resulting simply from applying hydrostatic pressure. The cement may also play a part since its behaviour may be like that of talc. The absence of similar pressure-release effects in the sodium chloride specimens also appears consistent since sodium chloride differs from calcite in being isotropic in its linear compressibility and more nearly isotropic in yield stress, while in no way resembling the model of an assemblage of hard particles which may to some extent represent the sandstone.

Interaction of volume change and stress–strain properties

In seeking to elucidate the mechanism of deformation of a material, account is often taken of the degree of resistance that it offers to deformation and of the way in which this changes with the nature and amount of the deformation and with changes in pressure and temperature. In tests where only one principal stress is non-zero ('uniaxial tests'), it is sufficient to specify this stress as measuring the resistance to deformation and so attention is directed to the stress–strain curve itself. However, under more general states of stress no single applied stress component is an adequate measure of the resistance of deformation. Instead, what is likely to be more relevant is the increment of work needed per increment of deformation.

In particular, in the 'triaxial test' the differential stress does not in general represent the rate at which work is being done within the specimen because of the work associated with volume change under the confining pressure. Assuming that the specimen axis is a principal axis of strain, the total work dW done on the specimen per unit volume during an increment of axial strain $d\epsilon_1$ in the triaxial test can be written [5, 17] as

$$dW = (\sigma + p)d\epsilon_1 + 2\,pd\epsilon_3$$

or

$$dW = \sigma d\epsilon_1 + pd\epsilon_v.$$

Here σ is the differential stress ($\sigma_1 - \sigma_3$ in conventional notation), p is the confining pressure (σ_3), $d\epsilon_3$ is the increment in radial strain and $d\epsilon_v$ is the increment in volumetric strain; we adopt the convenient sign convention that compressive stresses and strains are positive and that decrease in volume is also represented by positive volumetric strain ($d\epsilon_v = -dv/v$, analogous to $\epsilon = -dl/l$). Thus we can take as the measure of the resistance to deformation the parameter

$$\sigma_w = \frac{dW}{d\epsilon_1} = \sigma + p\,\frac{d\epsilon_v}{d\epsilon_1}. \qquad (1)\dagger$$

When the specimen is compacting, σ_w is higher than σ and when the specimen is dilating it is lower. The deformation itself is fully specified by ϵ_1 and ϵ_v but, when comparing behaviour in closely related triaxial tests, the plot of σ_w against ϵ_1 alone will often serve to characterize the stress–strain properties sufficiently for our purposes, especially when ϵ_1 is large compared with ϵ_v.

Two properties of the stress–strain behaviour that may be important in suggesting the nature of the deformation mechanism can now be expressed.

1. Work hardening. Defining work hardening as the change in resistance to deformation as the deformation proceeds, it can be derived from the triaxial test as

$$\frac{d\sigma_w}{d\epsilon_1} = \frac{d\sigma}{d\epsilon_1} + p\,\frac{d^2\epsilon_v}{d\epsilon_1{}^2}. \qquad (2)$$

When the volume changes linearly with strain, $d\sigma_w/d\epsilon_1$ is the same as $d\sigma/d\epsilon_1$, the apparent rate of work hardening from the σ vs ϵ_1 plot, but curvature in the volume change vs strain plot introduces an additional work-hardening component, as recognized by FRANK [18] and BRACE *et al.* [2]. Thus, the effective work-hardening rate is greater than $d\sigma/d\epsilon_1$ when the ϵ_v vs ϵ_1 plot is concave towards positive ϵ_v, that is, when $\Delta v/v_0$ vs ϵ_1 (as plotted here) is concave downwards, and it is less than $d\sigma/d\epsilon_1$ when $\Delta v/v_0$ vs ϵ_1 is concave upwards. Put in another way, even if the intrinsic resistance to deformation does not change with strain, a changing porosity during a triaxial test gives rise to an apparent work hardening in the σ vs ϵ_1 plot when $\Delta v/v_0$ vs ϵ_1 is concave upwards or an apparent work softening when $\Delta v/v_0$ vs ϵ_1 is concave downwards.

2. Pressure sensitivity. The influence of pressure on the intrinsic resistance to deformation at any particular strain ϵ_1 is correspondingly represented by

$$\left(\frac{d\sigma_w}{dp}\right)_{\epsilon_1} = \left(\frac{d\sigma}{dp}\right)_{\epsilon_1} + \frac{d}{dp}\left(p\,\frac{d\epsilon_v}{d\epsilon_1}\right)_{\epsilon_1} \qquad (3)$$

or

$$\tan\psi_w = \tan\psi + \frac{d}{dp}\left(p\,\frac{d\epsilon_v}{d\epsilon_1}\right)$$

where $\tan\psi$ is the slope of the $\sigma_{\epsilon,1}$ vs p curve, related to the slope $\tan\phi$ of the Mohr envelope for the stress state at given strain by [19]‡

$$\tan\phi = \frac{\tan\psi}{2\sqrt{(1+\tan\psi)}}.$$

† The corresponding expression for the shear test is

$$\frac{dW}{d\gamma} = \tau + \sigma_n\,\frac{d\epsilon_v}{d\gamma}$$

where $d\gamma$ is the increment in shear strain, and τ and σ_n are the shear stress and normal stress, respectively, on the shear plane.

‡ The use of $\tan\psi$ or $\tan\phi$ as an index of pressure sensitivity, as in this earlier paper, is only meaningful in the absence of significant volume changes.

Curves of $\sigma_w{}^*$ vs ϵ_1 for the six materials are given in Figs 3(b)–8(b). The addition of the asterisk superscript to σ_w indicates that in deriving these from the observations given in Figs 3(a), (c)–8(a), (c), respectively, the elastic volume changes due to the applied differential stresses were first subtracted from the measured $\Delta v/v_0$ vs ϵ_1 curves; that is, in applying equation (1) we have used $d\epsilon_{vp}/d\epsilon_1$ instead of $d\epsilon_v/d\epsilon_1$ where ϵ_{vp} is the non-elastic part of the volumetric strain. This ensures that the $p(d\epsilon_{vp}/d\epsilon_1)$ term reflects only the work associated with non-elastic volume changes and does not include elastic work which is recovered when the differential stress is removed. In deriving the elastic volumetric strains from the measured differential stresses, the elastic moduli used, which for isotropic material should be equal to one-third of the compressibility, have been chosen to be approximately consistent with the volume changes measured when the differential stress is released at the end of the straining, as indicated by the vertical lines at the ends of the curves of Figs 3(c)–8(c). These moduli are larger than correspond to the compliances of the mineral grains themselves since they take into account elastic changes in pore volume as well. The values used were $0{\cdot}0007\ \text{kb}^{-1}$ for limestone, marble and talc, $0{\cdot}001\ \text{kb}^{-1}$ for sandstone and $0{\cdot}0014\ \text{kb}^{-1}$ for sodium chloride, but, as the examples in Figs 3(c)–8(c) (dotted lines) show, the elastic corrections are generally not so large relative to the total volume changes as to make the choice of these values particularly critical. In the case of graphite where a single value for all experiments is no longer a sufficient approximation because of the effect of large changes of porosity from one pressure to another and even during one experiment, an interpolated set of moduli was used, given in Fig. 7(e) as a function of instantaneous porosity and ranging from $0{\cdot}007$ to $0{\cdot}002\ \text{kb}^{-1}$. Another approximation affecting the calculation of $\sigma_w{}^*$ is the use of conventional strains for both ϵ_1 and ϵ_v where, strictly, logarithmic strains should have been used, but within the limits of accuracy set by the data no serious error should arise from this.

It must be emphasized that the $\sigma_w{}^*$ vs ϵ_1 curves in Figs 3(b)–8(b) are of a rather imprecise nature, especially at low strains†, in view of the limited accuracy of the data and its effect on the measurement of slopes and of the other approximations mentioned above. Nevertheless, it is believed that the $\sigma_w{}^*$ vs ϵ_1 curves are a much better guide to the processes occurring in the specimen than are the σ vs ϵ_1 curves. We shall therefore now discuss the main features of the behaviour of the individual materials with reference to the $\sigma_w{}^*$ vs ϵ_1 curves.

Limestone and marble [Figs 3(b) and 4(b)]. The differences in behaviour of the two calcite rocks suggested by the σ vs ϵ_1 curves appear less marked in several respects when the interaction of the volume changes is allowed for. Thus, the limestone curves no longer cross over at low strains, supporting the earlier suggestion [11] that this effect on the σ vs ϵ_1 is associated with an increased contribution of pore collapse during straining at higher pressures. Also, the effective work hardening of the marble now appears comparable to or even rather higher than that of the limestone; the high slopes of the σ vs ϵ_1 curves for the limestone are therefore to be attributed to a large $p(d^2\epsilon_{vp}/d\epsilon_1{}^2)$ effect rather than to an intrinsically high work-hardening rate associated with the mechanism of deformation. However, the limestone still appears much the stronger; its $\sigma_w{}^*$ vs ϵ_1 curves in compression are generally at least 1 kb higher than those of the marble up to 4 kb confining pressure, with an increasing difference at higher pressures due to a higher pressure sensitivity of the limestone curves at the higher pressures.

† Little or no significance should be attached to the $\sigma_w{}^*$ vs ϵ_1 curves below about 1 per cent strain. Note that, in principle, they need not pass through the origin, the case of graphite being a possible example of this.

Sandstone [Fig. 5(b)]. As for the lithographic limestone, the apparent work hardening shown by the σ vs ϵ_1 curves is strongly affected by the $p(d^2\epsilon_{vp}/d\epsilon_1{}^2)$ term, the $\sigma_w{}^*$ vs ϵ_1 curves showing a sharper bending over and an earlier reaching of peak strength. There is also a more marked decline in strength with increasing strain beyond the peak (this would be even more accentuated if the extra increase in cross-sectional area due to barrelling were allowed for).

Talc [Fig. 6(b)]. In this case, the stress–strain curves are not greatly modified by allowing for volume-change effects, the increased pressure sensitivity shown in the $\sigma_w{}^*$ vs ϵ_1 plot being the most noticeable effect.

Graphite [Fig. 7(b)]. Volume changes are very important in graphite [15]. In particular, the apparent work hardening shown by the σ vs ϵ_1 curves is largely a volume-change effect, very little being shown in the $\sigma_w{}^*$ vs ϵ_1 curves except at small strains.

Sodium chloride [Fig. 8(b)]. Although the small volume changes that occur at each pressure are roughly equal, the $p(d^2\epsilon_{vp}/d\epsilon_1{}^2)$ term increases with pressure. Thus the $\sigma_w{}^*$ vs ϵ_1 curves reveal a small pressure sensitivity in the stress–strain behaviour which had been obscured in the σ vs ϵ_1 curves by the volume-change effect (for clarity, only the 0·25 and 8 kb curves are shown, the curves for other pressures falling in between).

Mechanisms of deformation

Intragranular deformation by the crystallographic gliding processes, slip and twinning, which accounts for the high ductility under ordinary conditions of such materials as polycrystalline copper or silver chloride, is known to be important in many rocks (see, for example, Griggs and Handin [20], Carter *et al.* [21] and Raleigh [22]). On the other hand, the deformation of rocks such as poorly-cemented sandstones often clearly involves the relative movement of grains, a process well-known in soils and usually referred to as flow of a 'granular material'. Such a process is thought also to play a part in the deformation of compact rocks where the available intragranular plasticity is inadequate, but it will have to be associated with widespread fracturing along grain boundaries and within grains ('microfracturing') so as to make possible the relative movement of the grains or their fragments; the term 'cataclastic flow' is used to refer to this combination of processes. Therefore, following Griggs and Handin [23], and ruling out change of shape by diffusional mass transport in the present context, we may expect the deformation of any rock to be accomplished by some combination of intragranular plasticity and cataclastic flow. The relative contributions of the two types of mechanism in a particular rock might be determined by detailed microscopic study but this is complicated by the additional changes in the rock during pressure release. Here we attempt to draw some conclusions from the volume change and stress–strain observations made during deformation at high pressure, using the following premises:

1. Volume change. When the initial porosity is zero, intracrystalline plasticity can be assumed to involve no volume change since, except under low-pressure creep conditions, any change from accumulation of crystal defects will be smaller than is measurable here, whereas in cataclastic deformation volume inevitably increases in order to accommodate the relative movement of grains or their fragments. However, when there is initial porosity, some ambiguity enters in the interpretation of volume changes. Dilatancy will usually indicate a component of cataclastic deformation if an effective confining pressure is present, otherwise unnecessary work would be done against the confining pressure (an exception to this may sometimes arise when an inadequacy of slip systems under von Mises's require-

ment for ductility can be compensated by heterogeneity of deformation involving the pores [10]). On the other hand, inelastic decrease in volume during deformation is not, in itself, uniquely diagnostic of either intracrystalline plasticity or cataclastic flow.

2. Pressure sensitivity. On present evidence [19, 24, 25] the resistance to intracrystalline gliding depends only slightly on pressure compared with the substantial pressure dependence in cataclastic flow introduced by the macroscopic friction involved. This difference should help to identify the predominant mechanism of deformation. However, in interpreting the observed stress–strain curves, the work involved in volume change under pressure must first be allowed for as above. The value of tan $\psi_w^* = d\sigma_w^*/dp$ at some particular strain ϵ_1 can then be taken as an index of the pressure sensitivity of the deformation processes themselves. At the extremes, pure intracrystalline plasticity can be expected to give a tan ψ_w^* of less than $0 \cdot 1$, commonly of the order of $0 \cdot 01$, while purely cataclastic deformation will give a tan ψ_w^* of the order of 1 or more for materials of average frictional properties (tan $\psi = 1$ corresponds to tan $\phi = 0 \cdot 35$).

The *sodium chloride* evidently deforms entirely by intracrystalline plasticity in view of the low-pressure sensitivity of its stress–strain curve (tan $\psi_w^* = 0 \cdot 02$) and the lack of dilatancy; the small compaction results from elimination of porosity without involving significant cataclasis. Presumably slip on cube or other non-(110) planes is involved since the normally-active (110) planes comprise only two independent slip planes, far short of the von Mises requirement of five (cf. the case of MgO [25]).

The behaviour of *Carrara marble* also lends itself to fairly clear interpretation because of the low initial porosity. The dilatancy and the substantial pressure dependence in compression tests at all pressures up to about 4 kb indicate that cataclastic flow is an important part of the deformation mechanism and that it has a predominating influence in determining the character of the deformation up to 2 kb (tan ψ_w^* greater than 1 at most strains in this pressure range). Only at pressures above 5 kb does the deformation appear to approximate pure intracrystalline plasticity (tan $\psi_w^* = 0 \cdot 05$ or less). This is probably because, although calcite has enough independent slip systems to satisfy von Mises's condition, the resolved shear stress for slip is relatively high [26] and so only at the highest pressures is it always easier than propagation of microfractures. The easily-produced twinning is inadequate for a general deformation [10] and so in itself does not determine the level of the stress–strain curve. Thus, although the macroscopic brittle–ductile transition in Carrara marble is around $0 \cdot 5$ kb, the transition to full intracrystalline plasticity is not completed until at least 4–5 kb at room temperature. The decrease in volume during deformation above 4 kb is presumably collapse of porosity that does not involve widely-distributed cataclasis.

In the *lithographic limestone*, the situation is complicated by the larger initial porosity. Although dilatancy is absent in compression tests above about 2 kb, the pressure sensitivity suggests that cataclastic flow largely determines the level of the stress–strain curve up to at least 4 kb and still plays some part up to 8 kb (tan ψ_w^* greater than 1 up to 4 kb and still not less than $0 \cdot 5$ at 8 kb). The compaction during deformation, especially in the 2–4 kb range, therefore presumably represents a partial removal of initial porosity while retaining enough free volume to accommodate the cataclastic processes; some porosity is still retained after 20 per cent deformation at 8 kb. The higher levels of the stress–strain curves and the greater difficulty of achieving full intracrystalline plasticity than in Carrara marble are probably mainly related to the finer grain size but possibly also to differences in purity. It should be emphasized that in neither material can we estimate the actual fractions of total strain contributed by the two types of processes, as distinct from discussing the degree to which each controls the course of the stress–strain curve and, in fact, intracrystalline plasticity may contribute a large part of the total strain over much of the ductile field.

The high-pressure sensitivity of the stress–strain curves of the *sandstone* ($\tan \psi_w^* = 1$–$1 \cdot 5$) points to its deformation being mainly cataclastic flow, like that of a granular mass of quartz and felspar (cf. quartz sand [4]), with the matrix cement apparently not greatly modifying the behaviour. However, the volume-change observations suggest that the sandstone does not conform to the picture, often discussed in soil mechanics [27, 28], of approach to a critical void ratio in the deformation of a granular medium. Here the situation must be complicated by continual changes in structure associated with comminution of grains and subsequent readjustments in their packing, these effects being somehow reflected in the general tendency to dilatancy at larger strains, accompanied by strain softening, after the preliminary phase of compaction.

Graphite and *talc* are both aggregates of a platy mineral in which intracrystalline slip is probably restricted to the unique cleavage plane. Such slip is inadequate for homogeneous deformation in the aggregate, even if kinking is taken into account, and so additional accommodating mechanisms are required [10]. For the latter, non-basal slip is likely to be too difficult and so some cataclastic flow can be expected. In talc, there is probably a component of cataclastic flow in all cases since $\tan \psi_w^*$ is about $0 \cdot 2$–$0 \cdot 3$ over the whole pressure range. In graphite, the situation is similar up to about 4 kb but at higher pressures $\tan \psi_w^*$ decrease to around $0 \cdot 05$. A possible explanation, which avoids postulating a marked decrease in coefficient of friction at high normal stresses or the activation of additional slip mechanisms, is that the deformation now occurs almost entirely by basal slip and that any incompatibility in strain from grain to grain is accommodated in the pore space, which is still appreciable compared with that in the talc at high pressures.

Extension tests

For the lithographic limestone at small strains, say below 5 per cent, the difference between the extension stress–strain curve at $6 \cdot 5$ kb and the compression curve at about the same pressure [Fig. 3(a)] can be mainly ascribed to the difference in work associated with volume change since the σ_w^* curves [Fig. 3(b)] more nearly coincide or even fall in reverse order (it must be borne in mind that the low precision of the derived curves, especially at low strains, permits only very approximate comparisons). The Carrara marble extension and compression curves [Fig. 4(a) and 4(b)], which are less influenced by volume changes at around $6 \cdot 5$ kb, nearly coincide at low strains in either plot. The large difference in mean stress between the extension tests and compression tests at the same confining pressure therefore evidently has little influence on the deformation processes at small strains at this level of pressure. However, the difference in mean stress does appear to be important at larger strains where for both materials the σ_w^* vs ϵ_1 curves in extension lack the intrinsic work hardening that appears in compression. This suggests that the cataclastic component in the deformation becomes more dominant in the extension tests as straining proceeds.

In neither material is the Mohr failure condition valid for the flow stress at a given strain since the Mohr envelopes for extension and compression tests will not coincide, irrespective of whether the early part or later part of the stress–strain curve is being considered. The Mohr theory predicts that the Mohr stress circle for an extension test with $6 \cdot 5$ kb as maximum compressive principal stress should coincide with that for a compression test with the same maximum compressive principal stress (this would be at about $1 \cdot 7$ kb confining pressure for the limestone and between 2 and $2 \cdot 5$ kb for the marble). However, the latter circle is always of smaller radius than the former, irrespective of whether σ or $\sigma_w{}^*$ is considered as flow stress. This means that, in effect, increase in the intermediate compressive principal stress σ_2 increases the level of the stress–strain curve in tests where the extreme principal stresses are in the vicinity of 2 and 6 kb, respectively.

BRITTLE–DUCTILE TRANSITION AND OTHER STABILITY ASPECTS

From the pressure-sensitivity of the flow stress and from the dilatancy, it is evident that the brittle–ductile transition is not simply a transition from macroscopic fracture to intracrystalline plasticity. Microcracking, known to be prevalent prior to macroscopic fracture [2, 29], must still be widespread and important above the transition [3]. The transition can therefore be said to be determined as the pressure above which microcrack propagation is stabilized at all strains, so that no individual microcrack or combination of them develops into a microscopic fracture. The stabilizing [30, 31] presumably results from factors such as plastic work ('plastic blunting'), the friction between sliding surfaces, or the difficulty of a crack crossing grain boundaries or other barriers such as other cracks. To describe the transition simply as the pressure at which 'the stress required to form a fault is equal to the stress to cause sliding on the fault' [32] does not bring out its essential nature. Rather, dealing with the transition in terms of stability or instability of crack propagation calls for concepts on the microscale analogous to those, such as critical strain energy release rate or critical crack size, developed in technical fracture mechanics [33, 34]; BIENIAWSKI [35] has already applied some of these notions to rocks on the larger scale.

Another stability question is whether, when the pressure is above the transition, the deformation within a uniformly loaded specimen will be uniformly distributed or will tend to be concentrated within localized zones such as shear bands (cf. Lüders' bands in mild steel). This should be decided by Drucker's criterion of material stability according to which, in the absence of a geometrical instability such as necking, a material will deform in a stable manner if 'additional deformation requires positive work by the external agency' [36]. In the present situation where some of the work is involved in volume change, this criterion predicts distributed or stable deformation when the σ_w vs ϵ_1 curves show work hardening and localized or unstable deformation where they show work softening. Our observations are consistent with this. In particular, the sandstone seems to deform uniformly, apart from the barrelling due to end-constraints, while the σ_w vs ϵ_1 curve is rising, but localization of deformation sets in after the curve bends over—although the experiments are not very critical in establishing an exact correlation here.

A possible explanation, in the case of porous rocks, for the ductile-to-brittle transition with increasing pressure of the type described by BYERLEY and BRACE [37] may also lie in an analogous effect if with increasing pressure the $\Delta v/v_0$ vs ϵ_1 curve develops a sufficiently marked upward curvature ($d^2\epsilon_v/d\epsilon_1{}^2$ negative) to produce an overall work softening in the σ_w vs ϵ_1 curve. The appearance of p in the $p(d^2\epsilon_v/d\epsilon_1{}^2)$ term in equation (2) leads to this term becoming more important at higher pressures even if $d^2\epsilon_v/d\epsilon_1{}^2$ is not changing markedly with pressure (note that it is only upward curvature of $\Delta v/v_0$ vs ϵ_1 that is relevant, not actual change from compaction to dilatation with increasing strain).

An alternative situation may arise, although not illustrated in our experiments, where there is volume change occurring such that $\Delta v/v_0$ vs ϵ_1 is concave downwards ($d^2\epsilon_v/d\epsilon_1{}^2$ positive). It is then possible for the σ_w vs ϵ_1 curve to show work hardening even though the σ vs ϵ_1 curve is falling. This could give rise to a situation where, in spite of a downward sloping stress–stress curve being observed, no localized shear develops, and so help explain the apparent lack of correlation between axial stress–strain behaviour and nature of deformation pointed to by GRIGGS and HANDIN [23].

It is not clear why, as observed above, barrelling appears more pronounced when the specimen dilates during deformation than when it compacts and further observations are needed to test whether this correlation is a general effect. Dilation contributes an additional lateral expansion which will tend to exaggerate the barrelling due to end-constraint but this is a minor effect. Otherwise, the explanation may involve a more far-reaching influence of the end-constraints in a dilating specimen.

Application

The main aim of this study has been the better understanding of fundamental mechanisms of rock deformation rather than immediate practical application and only some suggestions regarding applications can be made here. Points of relevance to solid-medium high-pressure apparatus have been discussed elsewhere [14]. Applications in engineering rock mechanics are likely to arise especially when pore fluids are present since dilatancy or compaction will lead to decrease or increase, respectively, in the pore pressure if the rates of strain relative to the permeability of the rock are such that a condition of 'incomplete draining' exists and this will influence any phenomena dependent on pore pressure. Also, roles of dilatancy in metamorphism, the generation of magma and the occurrence of earthquakes have been proposed by earlier writers [18, 38].

Application to geology is made difficult by lack of knowledge of the influence of higher temperature or slower strain rate, either of which will tend to reduce the role of cataclastic flow and dilatancy under geological conditions. However, they may still be present under low-grade conditions where the available crystallographic glide systems are inadequate for full intracrystalline plasticity and diffusion-dependent alternative processes are still relatively slow, or even under higher-grade conditions when the pore pressure is high. In such cases, inelastic volume changes of either sign may have important consequences. Dilatancy may facilitate movement of fluid phases in a rock of initially low permeability, thereby accelerating metasomatic or other metamorphic processes; this could be one of the most important ways in which mineralogical reactions are accelerated in deforming regions. The alternative effect of deformation in accelerating compaction in porous rock may be relevant in the compaction of sedimentary rocks.

It is possible that a dilatancy associated with deformation under upper crustal conditions occurs in the vicinity of active faults, for example, near the San Andreas Fault [39]. Such an association would imply that the straining in the vicinity of the fault is not a steady state process; it may be an aspect of episodic behaviour at the fault. A possible consequence, if the ratio of strain rate to permeability is appropriate, is a decrease in pore pressure at the fault, thereby inhibiting slippage on the fault itself and allowing a general build-up in stress levels.

Acknowledgement—WAYNE C. BURNHAM gave us the idea of using an unpotted LVDT inside the pressure vessel.

REFERENCES

1. BRIDGMAN P. W. Volume changes in the plastic stages of simple compression. *J. appl. Phys.* **20,** 1241–1251 (1949).
2. BRACE W. F., PAULDING B. W. JR. and SCHOLZ C. Dilatancy in the fracture of crystalline rocks. *J. geophys. Res.* **71,** 3939–3953 (1966).
3. SCHOLZ C. H. Microfracturing and the inelastic deformation of rock in compression. *J. geophys. Res.* **73,** 1417–1432 (1968).

4. Borg I., Friedman M., Handin J. and Higgs D. V. Experimental deformation of St. Peter sand: a study of cataclastic flow. *Mem. geol. Soc. Am.* **79,** 133–191 (1960).
5. Handin J., Hager R. V. Jr, Friedman M. and Feather J. N. Experimental deformation of sedimentary rocks under confining pressure: pore pressure tests. *Bull. Am. Ass. Petrol. Geol.* **47,** 717–755 (1963).
6. Brace W. F. and Orange A. S. Electrical resistivity changes in saturated rocks during fracture and frictional sliding. *J. geophys. Res.* **73,** 1433–1445 (1968).
7. Mises R. von Mechanik der plastischen Formändering von Kristallen. *Z. angew. Math. Mech.* **8,** 161–185 (1928).
8. Taylor G. I. Plastic strain in metals. *J. Inst. Metals* **62,** 307–324 (1938).
9. Groves G. W. and Kelly A. Independent slip systems in crystals. *Phil. Mag.* **8,** 877–887 (1963).
10. Paterson M. S. The Ductility of Rocks, in *Physics of Strength and Plasticity* (Ali S. Argon, Ed.) pp. 377–392, M.I.T. Press, Cambridge (1969).
11. Paterson M. S. Triaxial testing of materials up to 10,000 kg/sq.cm. *J. Instn Engrs Aust.* **36,** 23–29 (1964).
12. Vesic A. S. and Clough G. W. Behaviour of granular materials under high stresses. *J. Soil Mech. Fdns Div. Am. Soc. civ. Engrs* **94,** (SM3) 661–688 (1968).
13. Bishop A. W. The strength of soils as engineering materials. *Géotechnique* **16,** 91–128 (1966).
14. Edmond J. M. and Paterson M. S. Strength of solid pressure media and implications for high pressure apparatus. *Contr. Mineral. Petrol.* **30,** 141–160 (1971).
15. Edmond J. M. and Paterson M. S. Effects of pressure on the deformation of graphite. *Carbon.* In press.
16. Paterson M. S. Secondary changes of length with pressure in experimentally deformed rocks. *Proc. R. Soc.* **A271,** 57–87 (1963).
17. Bishop A. W. Discussion. *Géotechnique* **4,** 43–45 (1954).
18. Frank F. C. On dilatancy in relation to seismic sources. *Rev. Geophys.* **3,** 485–503 (1965).
19. Paterson M. S. Effect of pressure on stress–strain properties of materials. *Geophys. J.R. astr. Soc.* **14,** 13–17 (1967).
20. Griggs D. and Handin J. (Ed.) Rock Deformation (A Symposium). *Mem. geol. Soc. Am.* **79** (1960).
21. Carter N. L., Christie J. M. and Griggs D. T. Experimental deformation and recrystallization of quartz. *J. Geol.* **72,** 687–733 (1964).
22. Raleigh C. B. Glide mechanisms in experimentally deformed minerals. *Science* **150,** 739–741 (1965).
23. Griggs D. and Handin J. Observations on fracture and a hypothesis of earthquakes. *Mem. geol. Soc. Am.* **79,** 347–364 (1960).
24. Davis L. A. and Gordon R. B. Pressure dependence of plastic flow stress of alkali halide single crystals. *J. appl. Phys.* **39,** 3885–3897 (1968).
25. Paterson M. S. and Weaver C. W. Deformation of polycrystalline MgO under pressure. *J. Am. ceram. Soc.* **53,** 463–471 (1970).
26. Turner F. J., Griggs D. T. and Heard H. Experimental deformation of calcite crystals. *Bull. geol. Soc. Am.* **65,** 883–934 (1954).
27. Taylor D. W. *Fundamentals of Soil Mechanics,* Wiley, New York (1948).
28. Schofield A. and Wroth P. *Critical State Soil Mechanics,* McGraw-Hill, London (1968).
29. Mogi K. Study of elastic shocks caused by the fracture of heterogeneous materials and its relations to earthquake phenomena. *Bull. Earthq. Res. Inst. Tokyo Univ.* **40,** 125–173 (1962).
30. Dower R. J. On the brittle–ductile transition pressure. *Acta Met.* **15,** 497–500 (1967).
31. François D. and Wilshaw T. R. The effect of hydrostatic pressure on the cleavage fracture of polycrystalline materials. *J. appl. Phys.* **39,** 4170–4177 (1968).
32. Byerlee J. D. Brittle–ductile transition in rocks. *J. geophys. Res.* **73,** 4741–4750 (1968).
33. Irwin G. R. and Kies J. A. Fracturing and fracture dynamics. *Weld. J. Res. Suppl.* **31,** 95S–100S (1952).
34. Gurney C. and Hunt J. Quasi-static crack propagation. *Proc. R. Soc.* **A299,** 508–524 (1967).
35. Bieniawski Z. T. Stability concept of brittle fracture propagation in rocks. *Engng Geol.* **2,** 149–162 (1967).
36. Drucker D. C. Plasticity, in *Proceedings of the First Symposium on Naval Structural Mechanics* (J. N. Goodier and N. J. Hoff, Eds) pp. 407–451, Pergamon Press (1960).
37. Byerlee J. D. and Brace W. F. High-pressure mechanical instability in rocks. *Science* **164,** 713–715 (1969).
38. Mead W. J. The geologic role of dilatancy. *J. Geol.* **33,** 685–698 (1925).
39. Raleigh C. B. and Burford R. O. Tectonics of the San Andreas fault system. Strain studies. EOS *Trans. Am. geophys. Un.* **50,** 380–381 (1969).